EPJ Web of Conferences **196**, 00051 (2019) https://doi.org/10.1051/epjconf/201919600051
AVTFG2018

Numerical simulation of flow in triangular minichannel

Nikolay Sibiryakov [1,2,*], *Oleg* Kabov [1,2], and *Valentin* Belosludstev [1,2]

[1] Kutateladze Institute of Thermophysics SB RAS, 630090, Novosibirsk, Russia
[2] Novosibirsk State University, 630090, Novosibirsk, Russia

Abstract. Minichannel cooling systems show great potential for small scale electronics. In this paper we analytically and numerically investigate flow with evaporation in open triangular minichannels without upper gas flow. It models processes either in a groove or in an individual channel. From the laws of mass, momentum and energy conservation we derive equations for mean velocity and for the depth of the liquid. These equations have been solved numerically. The viscosity limits maximum fluid speed and causes the formation of dry spots. The heat flux reaches 40kW/m^2 for initial liquid velocity 2 m/s. It is demonstrated that triangular or grooved channels even without upper gas flow are perspective for cooling systems.

1 Introduction

Computer performance depends on processor frequency. Modern chips perform more than billion operations per second. Air fans struggle to absorb heat from personal computers and consume enormous amount of energy. Continued frequency increase requires basically new cooling systems that would be capable to dispel a remarkable amount of heat in a small area.

Minichannel cooling systems show great potential for miniature devices. Liquid or liquid-gas mixture flows require much less energy than air-based systems because fluids are better heat conductors than gases. One of the most effective channel cross-section is triangular. This shape has the maximum ratio of the surface area to the volume. System of such channels absorbs up to 500kW/m2 [1,2,3,4].

The efficiency of the minichannels increases if a liquid freely evaporates. The gas carries away external heat and cools the fluid surface. Moreover, grooving the surface of the channel significantly enhances heat transfer. When the liquid flows in triangular channel and evaporates, the depth decreases. Thus, the pressure drops and the fluid is sucked into the channel; hence, the heat absorption is enhanced.

The articles on this theme describe flow in horizontal channels [5,6]. In this work [5] the authors investigate condensation of water vapor on the walls of a channel. The gas flows with high velocity in the center of the channel. Thus, the water velocity is also initially high.

[*] Corresponding author: kolyasibir@yandex.ru

Peles and Haber [6] investigated heat transfer in a boiling stream of water in an enclosed channel. They also assume that the gas flows quickly above the liquid.

In this work, we investigate flow with evaporation in open triangular channel with a slight incline. These models process either in a groove or in an individual channel. The liquid is driven only by internal forces and gravity. Thus, this cooling system does not require an additional gas pump.

2 Theoretical model

The channel has triangular cross-section with the apex angle $\phi = \pi/6$ (Fig. 1, Fig. 2).

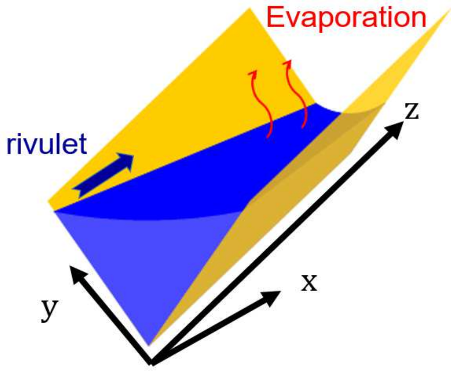

Fig. 1. The scheme of the channel.

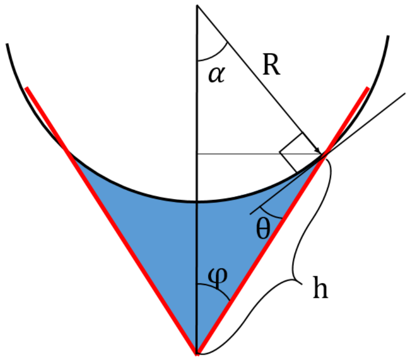

Fig. 2. Cross-section of the channel. Wetted length on the side of the channel is *h*.

The width of liquid film is less than 1 mm, so the temperature of the fluid is almost constant and equal to the temperature of the walls. Evaporation is proportional to the temperature of the liquid:

$$\mathrm{d}m = -\mathrm{C}(T)\,\mathrm{d}S \tag{1}$$

dm is evaporated mass, C(T) is the evaporation rate, T is the temperature of the fluid, dS is liquid surface area.

The capillary pressure P in the fluid: $P = P_0 - \sigma/R$. where σ is surface tension coefficient, R is the radius of curvature.

From geometric consideration (Fig. 2) we derive relations between different parameters of the liquid in the channel.

$$R = h \sin\phi/\cos(\phi+\theta) \tag{2}$$

$$\alpha = \pi/2 - \phi - \theta \tag{3}$$

where θ is the contact angle of the fluid and the surface of the channel.

The impulse flux in integral representation:

$$\int \rho \mathbf{g}\,\mathrm{d}V + \int (P - \zeta\,\rho v^2/2)\,\mathrm{d}\mathbf{S} = \int \rho \mathbf{v}(\mathbf{vn})\mathrm{d}S \tag{4}$$

The first integral is gravitational force. In the second integral negative term represents friction force between rivulet and the walls of the channel.

The equation for the averaged velocity ($v = v_z$, $v_x = 0$, $v_y = 0$), combining with the equation for evaporation, form a full system. Because the velocity and the depth of the liquid in our model depends only on z coordinate, we introduce ' = d/dz (v' = dv/dz, h' = dh/dz) and g_z is the projection of **g** on the z axis. Thus, from the above equations we get:

$$(vS)' = - h\alpha\, C(T)\sin\phi /[\rho \cos(\phi+\theta)] \tag{5}$$

$$(v^2S)' \rho/S = - P'+\rho g_z - \zeta(\rho v^2)\, L/2S \tag{6}$$

Where L is wetted diameter ($L = 2h$), S is liquid cross-section area.

$$S = h^2[\sin\phi - (\alpha - \sin\alpha) \sin^2\phi/\cos^2(\phi + \theta)] \tag{7}$$

Deriving v' and h' to get final system:

$$v' = [g_z + (\sigma A) / (2\rho v h^2) - (B/h - 2Ak)\, v/h] / (v - \sigma / 2\rho v h k) \tag{8}$$

$$h' = -A \sin\phi / [\mathrm{v} \cos(\phi+\theta)] - v'h / 2v \tag{9}$$

Where

$$k = R/h = \sin\phi/\cos(\phi+\theta) \tag{10}$$

$$A = \mathrm{C}(T)\, \alpha \tag{11}$$

$$B = 26.6\nu\, h^4/S^2 \tag{12}$$

This system of two ordinary differential equations describes the flow in the channel.

To solve the system, we used the 4th order Runge-Kutta method. It has a high precisions and slowly accumulate computational errors. The calculation area split in 10^4 steps. The simulation stops, when the velocity reaches critical limit:

$$2\rho v^2 = \sigma/R. \tag{13}$$

At this point velocity derivative tends to infinity and numerical modeling cannot accurately describe the processes in the channel. At a real experiment the capillary forces may collapse the liquid film and form a dry spot due to Plateau–Rayleigh instability.

3 Results and discussion

The depth of the liquid monotonously drops along the channel and, at the critical point (13) simulation stops (Fig. 3).

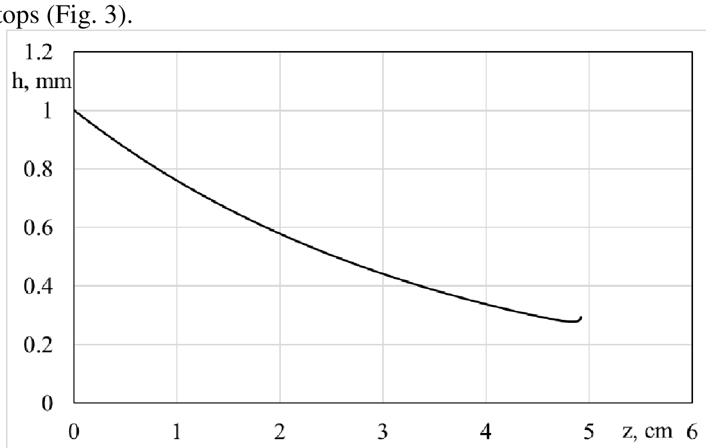

Fig. 3. The depth of the water along the channel. Initial velocity 2 m/s.

The velocity initially increased. After the apex friction forces overcame capillary, and the velocity dropped to the critical value (Fig. 4).

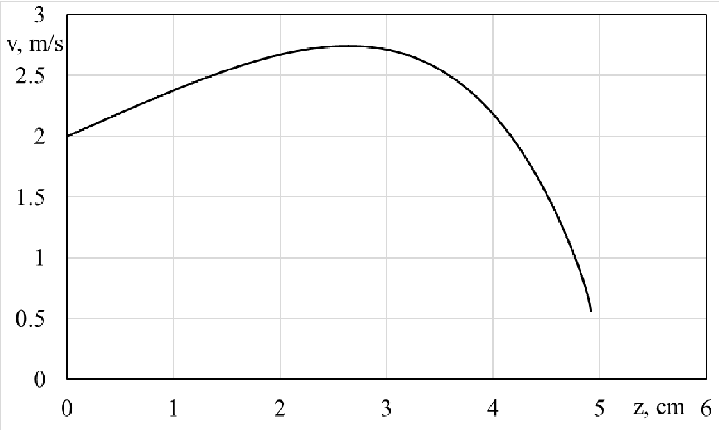

Fig. 4. The velocity of the water along the channel. Initial depth is 1 mm.

The effective heat flux in such a small channel is almost constant and equal 40 kW/m^2 (Fig. 5).

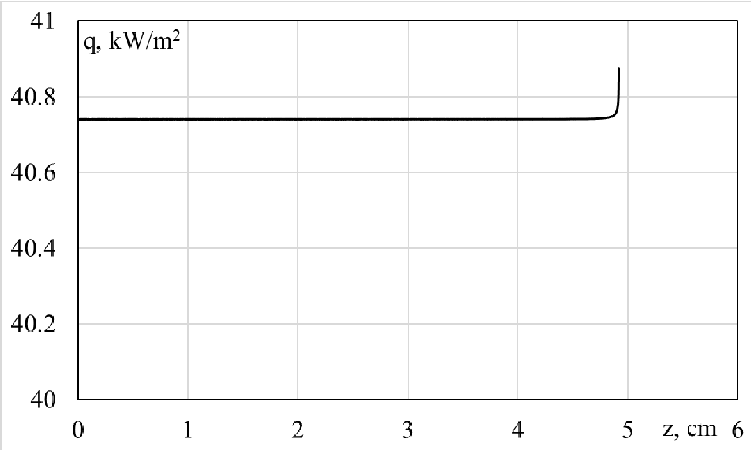

Fig. 5. The heat flux along the channel. Initial depth is 1 mm, initial velocity is 1 m/s.

At the end of the channel the velocity drastically decreases; thus, mass flow also rapidly decreases. Because the heat flux is proportional to evaporated mass, it sharply rises.

The non-viscous fluid never reaches critical limit (13) because the velocity limitlessly rises as the liquid flow along the channel; however, at some point either film evaporates completely or the velocity and depth reaches some point, where different physics starts.

4 Conclusions

As numerical simulation shows, capillary forces in minichannels increase effective cooling length and prevent dry spots appearance. However, viscosity limits maximum velocity and prevents films from quick thinning.

The simulation works until the velocity reaches critical value (13). In a real experiment Plateau–Rayleigh instability could grow and form a dry spot.

In non-viscous fluids the velocity limitlessly grows and never reaches a critical value.

Even without upper air flow small triangular channels effectively cool surfaces, absorbing about 40 kW/m^{2}heat flux.

The research was supported by RSF (project No. 18-79-10258).

References

1. E.Ya. Gatapova, O.A. Kabov, International Journal of Heat and Mass Transfer, **51** (2008)
2. I. Tiselj, G. Hetsroni, B. Mavko, A. Mosyak, E. Pogrebnyak, Z. Segal, International Journal of Heat and Mass Transfer, **47** (2004)
3. T.S. Zhao, Q. Liao, International Journal of Heat and Mass Transfer, **45** (2002)
4. G.P Peterson, H.B. Ma, ASME J. Heat Transfer, **118**, p. 731–739 (1996)
5. T.S. Zhao, Q.C. Bi, International Journal of Heat and Mass Transfer, **44** (2001)
6. Y.P. Peles, S. Haber, International Journal of Multiphase Flow, **26** (2000)